

RESEARCH ARTICLE | MAY 30 2023

# Study of Ouw natural clay Ouw-TiO<sub>2</sub> manufacturing methods for applications in the degradation reaction of linear alkylbenzene sulfonates

Thamrin Azis; Muhammad Nurdin; Muhammad Zakir Muzakkar; ... et. al



AIP Conference Proceedings 2704, 030005 (2023)

<https://doi.org/10.1063/5.0138598>



View Online



Export Citation

CrossMark

## AIP Advances

Why Publish With Us?

-  **25 DAYS**  
average time to 1st decision
-  **740+ DOWNLOADS**  
average per article
-  **INCLUSIVE**  
scope

[Learn More](#)



# Study of Ouw Natural Clay Ouw –TiO<sub>2</sub> Manufacturing Methods for Applications in the Degradation Reaction of Linear Alkylbenzene Sulfonates

Thamrin Azis<sup>1, a)</sup>, Muhammad Nurdin<sup>1, b)</sup>, Muhammad Zakir Muzakkar<sup>1, c)</sup>,  
Wa Ode Nining<sup>1, d)</sup>, Laode A. Kadir<sup>1, e)</sup>, Imran<sup>1, f)</sup>, T. Wahidah<sup>1, g)</sup>, and  
Catherina M. Bjang<sup>2, h)</sup>

<sup>1</sup>Department of Chemistry, Faculty of Mathematics and Natural Sciences, Halu Oleo, University, Kendari 93231, Indonesia

<sup>2</sup>Department of Chemistry, Faculty of Mathematics and Natural Sciences, Pattimura University, Ambon 94321, Indonesia

<sup>a)</sup>Thamriazis06@gmail.com

<sup>b)</sup>mnurdin06@yahoo.com

<sup>c)</sup>zakir1703@yahoo.com

<sup>d)</sup>niningwaode@gmail.com

<sup>e)</sup>Kadir20512048@gmail.com

<sup>f)</sup>imranlaimu@gmail.com

<sup>g)</sup>Anditenri07@gmail.com

<sup>h)</sup>corresponding author: rienabijang@yahoo.com

**Abstract.** Research has been carried out to study the method of making TiO<sub>2</sub> Ouw natural clay composites and photocatalytic applications in the degradation reaction of Linear Alkylbenzene Sulfonate surfactants. The method used is the method of impregnation and pillarization. Calcination temperature studies were also carried out. The temperature variations used were 200, 250 and 300°C. Characterization was carried out using X-ray diffraction. The characterization results showed that the pillarization method at a temperature of 250°C had the highest peak of montmorillonite-TiO<sub>2</sub> phase while in the impregnation method gives the highest phase peak at the application of a calcination temperature at 200°C. The LAO-TiO<sub>2</sub> composite with the pillarization method at 250°C succeeded in degrading the Linear Alkylbenzene Sulfonate surfactant by 89.2% with an adsorption capacity of 0.357 mg/g, while the LAO-TiO<sub>2</sub> composite with the calcination temperature impregnation method of 200°C degraded the Linear Alkylbenzene Sulfonate surfactant by 80.75% with an adsorption capacity of 0.323 mg/g.

## INTRODUCTION

Clay is a natural mineral from the silicate group in which its availability is quite abundant in Indonesia. The distribution of clay in Maluku is generally in the areas of Ambon Island and Saparua (Ouw Village). Ouw Natural Clay (LAO) contains montmorillonite components[1]. Natural clay needs to be activated to increase the surface area[2]. Until now, several methods have been developed in the process of modifying natural clay, including impregnation and pillarization. The impregnated clay will have a large surface area. Sterte (1986) said that the use of metal oxide TiO<sub>2</sub> as a pillaring agent will increase the Bacal spacing of the clay and metal oxides will be

distributed in the pillared clay layer. The use of metal oxide  $\text{TiO}_2$  will increase the acidity of the clay[3]. The metal that is carried on the clay by impregnation will make the metal bifunctional. Ti-pillared clay will have a larger pore size, heat stable properties, have higher acidity and surface area compared to other metal oxide pillars and have high photocatalytic activity [4].

Detergents are synthetic cleaners made from petroleum-derived ingredients. Detergent is one product that is currently widely used, especially in households because of its ability to clean. One of the constituent components of detergents is a surfactant. The advantage of detergent lies in its surfactant which functions to lower the surface tension of the water so that it can release adhering dirt[5]. The detergent waste are disposed of on riverbanks or absorbed by the soil to accumulate in groundwater. Several studies have stated that detergents can be carcinogenic and cause unpleasant odors in drinking water. Contaminated water if consumed will be harmful to the body. The same effect will occur if the detergent foam that accumulates in the rivers covers the surface of the water so that it inhibits the penetration of sunlight and oxygen into the water resulting in disrupted aquatic life[6].

In the LAS degradation process, bacteria of the genus *Pseudomonas* can be used under anaerobic conditions which can degrade up to 74.29% with a contact time of 28 days[7]. The optimum contact time to use magnetite is 60 minutes with the optimum concentration of  $2.44 \times 10^{-6}$  mol/L. In another study, it was stated that degradation using a  $\text{TiO}_2$  catalyst gave the best results with a removal of 84.98% within 4 hours[8]. In this study, the effect of the manufacturing method on the adsorption ability of methylene blue dye was studied.

## MATERIALS AND METHODS

### Research Material

Ouw natural clay, Aquades, NaCl (pa Merck),  $\text{AgNO}_3$  (pa Merck),  $\text{H}_2\text{SO}_4$  (pa Merck),  $\text{BaCl}_2$  (pa Merck),  $\text{TiO}_2$  (pa Merck),  $\text{TiCl}_4$  (pa Merck), Absolute Ethanol (pa Merck), Linear Surfactant Alkylbenzene Sulfonate (pa Merck),  $\text{H}_2\text{O}_2$  (pa Merck), Methylene Blue (pa Merck), Chloroform (pa Merck), Whatman filter paper No. 42

### Research Procedure

#### *Sample Preparation*

Ouw's natural clay is washed with distilled water several times, then filtered to obtain clay that is completely free of impurities such as sand, gravel, and plant roots. After washing, the clay was dried for 2 hours in an oven at  $120^\circ\text{C}$ . The dried samples were ground and sieved using a 100 mesh sieve.

#### *Saturation using NaCl*

Take as much as 200 g of clay then dispersed it into 500 mL of 3 M NaCl solution while stirring for 24 hours. The clay was then filtered and the residue obtained was washed with distilled water several times until the filtrate did not produce a white precipitate with  $\text{AgNO}_3$ . After washing, the precipitate was dried in an oven at  $100^\circ\text{C}$ . The dry clay was ground until smooth and then sieved using a 100 mesh sieve.

#### *Activation using $\text{H}_2\text{SO}_4$*

Take 50 g of clay that has been saturated with NaCl then add 100 mL of 2 M  $\text{H}_2\text{SO}_4$  while stirring. The activation process was carried out for 24 hours, then filtered and the residue obtained was washed with distilled water until the filtrate did not produce a white precipitate. The clay is dried in an oven at a temperature of  $110$ – $120^\circ\text{C}$ [2].

#### *Pillarization using $\text{TiCl}_4$*

The manufacture of pillared clay begins with the manufacture of a pillar solution. The solution was prepared by mixing 50 mL of  $\text{TiCl}_4$  with 100 mL of ethanol which was stirred until the solution was homogeneous. A total of

50 mL of  $\text{TiCl}_4$ -Ethanol solution was mixed with 250 mL of distilled water and stirred for 3 hours. The solution that has been prepared is then added little by little to a suspension of 20 g of clay in 1000 mL of water (2%) and stirred for 20 hours. The suspension was then centrifuged, put into a filter and washed with distilled water until the filtrate did not produce a white precipitate with  $\text{AgNO}_3$ . The clay was dried in an oven at  $110^\circ\text{C}$  for 2 hours, ground and sieved using a 100 mesh sieve. Then it was calcined at 200, 250, and  $300^\circ\text{C}$  for 4 hours. Characterization is done using X-ray Diffraction [9].

#### *Impregnation Using*

As much as 25 g of activated clay, 3.33 g of  $\text{TiO}_2$  and 25 mL of ethanol were added while stirring with a magnetic stirrer for 4 hours. The clay was dried in an oven at  $110^\circ\text{C}$  for 2 hours, crushed and sieved using a 100 mesh sieve, then calcined at various temperatures of 200, 250, and  $300^\circ\text{C}$  for 5 hours. Characterization is done using X-ray diffraction.

#### *Surfactant degradation*

Linear Alkylbenzene Sulfonate (LAS) Solution 1000 mg/L 0.25 g of LAS is weighed then put into a 250 mL volumetric flask and diluted with distilled water until it reach the mark.

#### *Linear Alkylbenzene Sulfonate (LAS) Solution 10 mg/L*

For 1 mL of LAS standard solution was put into a 100 mL volumetric flask and diluted with distilled water until it reach the limit mark [10].

#### *Methylene Blue (MB) 100 mg/L*

A total of 100 mg MB was dissolved with distilled water in a 100 mL volumetric flask until it reach the limit mark. Take 30 mL of MB solution and put into a 1000 mL volumetric flask, add 500 mL and 41 mL of 3M  $\text{H}_2\text{SO}_4$  solution. Shake until it dissolved and then diluted until it reach the mark with distilled water.

#### *Optimum Wavelength Determination*

In the 2.5 mL LAS standard solution was put into a 50 mL volumetric flask and then diluted with distilled water until it reach the mark. The solution was then transferred into a 300 mL separatory funnel, added 5 mL of MB and extracted with 5 mL of chloroform. The chloroform layer on the bottom was taken and analyzed by UV-Vis spectrophotometer. The color absorbance extracted from the LAS standard solution was measured with chloroform as a blank at a wavelength of 500–750 nm [10].

#### *Calibration curve creation*

LAS standard solution was prepared with a 1.0 pipette; 2.0; 4.0; 6.0; 8.0 ; 10; and 20.0 mL of 10 mg/L LAS, put into a 50 mL volumetric flask and then diluted with distilled water until it reach the mark. The solution was then transferred into a 300 mL separatory funnel. 5 mL of MB was added and extracted with 5 mL of chloroform. The chloroform layer on the bottom was taken and analyzed by UV-Vis spectrophotometer. The color absorbance extracted from the LAS standard solution was measured using chloroform as a blank at the optimum wavelength.

#### *Surfactant degradation with Pillarized Clay using $\text{TiCl}_4$*

LAS solution was extracted as much as 10 mL then put into four Erlenmeyer pieces and added with 0.1 mL of  $\text{H}_2\text{O}_2$  each. To the first Erlenmeyer was added with 50 mg of  $\text{TiCl}_4$ -pillared clay without calcination, the second Erlenmeyer was added with 50 mg of  $\text{TiCl}_4$ -pillared clay at  $200^\circ\text{C}$ , the third Erlenmeyer was added with 50 mg of  $\text{TiCl}_4$ -pillared clay at  $250^\circ\text{C}$ , the fourth Erlenmeyer was added with 50 mg of  $\text{TiCl}_4$ -pillared clay at  $300^\circ\text{C}$  (samples were coded LP 0, LP 200, LP 250 and LP 300, respectively). The degradation process was carried out in a UV reactor for 60 minutes. Then the suspension was filtered and the absorbance of the filtrate was measured using a UV-Vis spectrophotometer at the optimum wavelength.

LAS solution extracted as much as 10 mL then put into four Erlenmeyer pieces and added with 0.1 mL of H<sub>2</sub>O<sub>2</sub> each. In the first Erlenmeyer, it was added with 50 mg of impregnated TiO<sub>2</sub> clay without calcination, the second Erlenmeyer was added with 50 mg of impregnated TiO<sub>2</sub> clay at 200°C, the third Erlenmeyer was added with 50 mg of impregnated TiO<sub>2</sub> clay at 250°C, the fourth Erlenmeyer was added with 50 mg of impregnated TiO<sub>2</sub> clay at 300°C (samples were coded LT 0, LP 200, LP 250 and LP 300, respectively). The degradation process was carried out in a UV reactor for 60 minutes. Then the suspension was filtered and the absorbance of the filtrate was measured using a UV-Vis spectrophotometer at the optimum wavelength.

## RESULT AND DISCUSSION

### Saturation with NaCl

The saturation of clay using 3 M NaCl aims to unify the cations in the clay interlayer with Na<sup>+</sup> ions. The Na<sup>+</sup> ion is most often used in the clay saturation process because Na-Monmorillonite has the ability to expand more easily. The uniformity reaction can be seen in the reaction below.



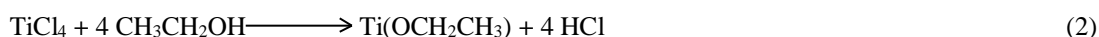
The above reaction explains the occurrence of cation exchange reactions other than Na<sup>+</sup> (Ca<sup>+</sup>, Mg<sup>2+</sup>, K<sup>+</sup> and so on) which aims to open and activate the space between the montmorillonite layers. Thus, it is expected that most of the cations other than Na<sup>+</sup> can be replaced by Na<sup>+</sup> cations so that the saturation process can facilitate the activation, impregnation, and pillarization processes.

### Activation using H<sub>2</sub>SO<sub>4</sub>

H<sup>+</sup> ions from H<sub>2</sub>SO<sub>4</sub> can reduce Na<sup>+</sup>, Ca<sup>+</sup>, and K<sup>+</sup> ions in the interlayer, besides the use of 2 M sulfuric acid is able to dissolve organic and inorganic impurities that cannot be dissolved by NaCl at the time of saturation [2,11], suggested that the most optimum clay activation was using a concentration of 2 M sulfuric acid because it did not damage the clay lattice. The activation process can also increase the active sites on the clay surface. And can increase the surface area so that clay can be used as a good catalyst support. While the use of sulfuric acid concentration that is too high can dissolve Al, Fe, and Mg in octahedral layers so that it can damage the clay lattice.

### Pillarization using TiCl<sub>4</sub>

Modification of clay is carried out by the pillarization method using a TiCl<sub>4</sub> pillaring agent, starting by mixing 50 mL of TiCl<sub>4</sub> with 100 mL of ethanol, while stirring until it produce a Ti-Polyhydroxy complex compound (Ti(OEt)<sub>4</sub>), the reaction that occurs according to [12,13] is



During the reaction, HCl gas is produced which smells very pungent. This reaction is an exothermic reaction. In this reaction, Ti(OCH<sub>2</sub>CH<sub>3</sub>)<sub>4</sub>, the shape of the structure of Ti(OCH<sub>2</sub>CH<sub>3</sub>)<sub>4</sub> shows that each Ti atom has 6 coordination bonds as shown in Fig. 1.

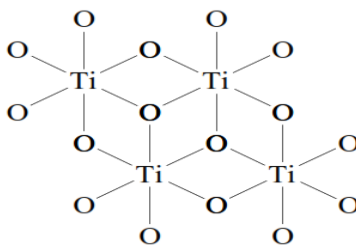


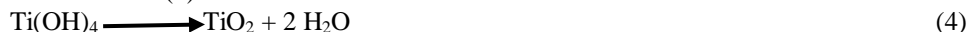
FIGURE 1. Structure of [Ti(OCH<sub>2</sub>CH<sub>3</sub>)<sub>4</sub>] (only Ti and O atoms are shown)

The addition of distilled water is done so that hydrolysis occurs and  $\text{Ti}(\text{OH})_4$  is formed as shown in reaction (3) according to [11]. Stirring aims to homogenize the solution which is characterized by the loss of  $\text{HCl}$  gas and a yellow solution.



Prior to the intercalation of the pillar solution on the clay, a suspension of clay and aquadest was made by mixing 20 g of clay in 1000 mL of distilled water (2%) then stirred for 20 hours. Intercalation is done drop by drop so that  $\text{Ti}(\text{OH})_4$  is intercalated in the clay interlayer area. The suspension was then centrifuged to separate the clay solids. Furthermore, the clay is washed until it's free of  $\text{Cl}^-$ . Subsequently, the calcination process was carried out at temperatures of 200, 250, and 300°C.

The intercalation stage is the stage where the oligomer will replace the position of the cations in the clay interlayer region. This can happen because the bonds that occur between clay layers are relatively weak. The negative charge on the clay layer will be a driving force for electrostatic interactions between the clay layers. The presence of water molecules that hydrate the cations in the interlayer region is able to keep the clay layer separate so that it will be easy for the Ti-Polyhydroxy complex to replace the cations. The calcination process aims to change the intercalated complex compound  $\text{Ti}(\text{OH})_4$  into titanium dioxide ( $\text{TiO}_2$ ) pillars in the clay interlayer. The calcination process, as shown in reaction (4).



While the variation of calcination temperature aims to determine the thermal stability of the pillared clay (not collapsed ones) against its photocatalytic ability. The results of calcination with the pillarization method using  $\text{TiCl}_4$  visually appear to change color at various variations in calcination temperature. Pillared clay without calcination temperature looks brownish compared to the calcination temperature of 200°C which has a grayish color and changes back to slightly brownish at 250°C. The higher the calcination temperature, the more gray the color of the clay will be. This is because the calcination temperature affects the components in the pillared clay.

## Characterization

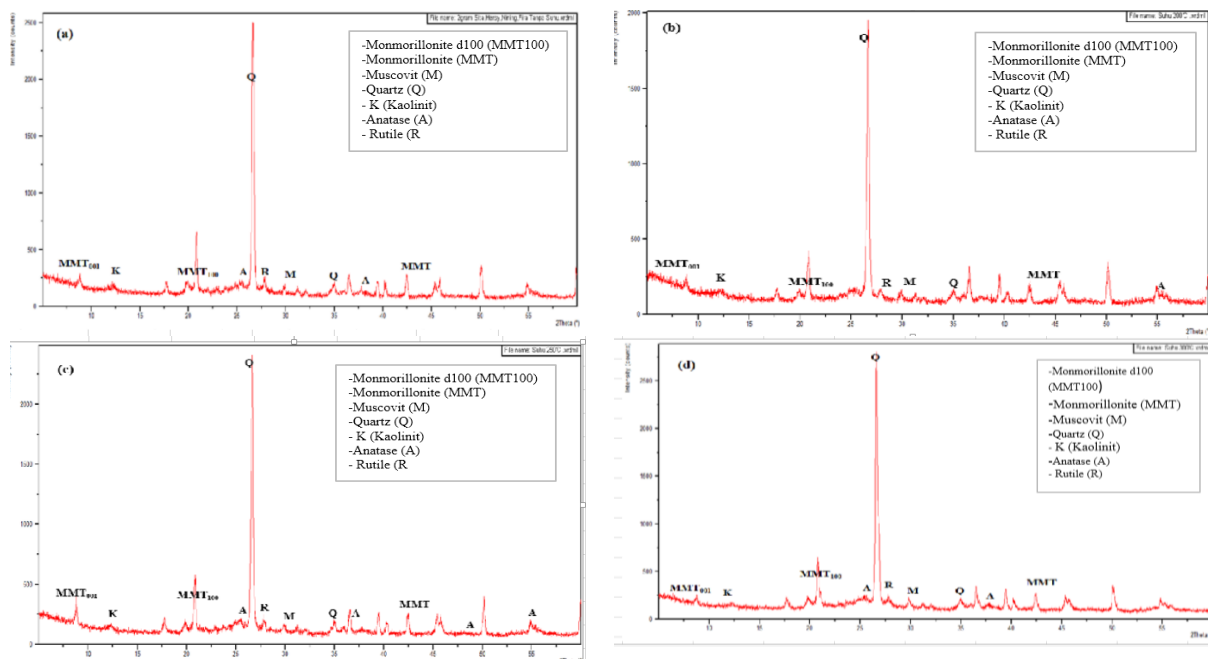


**FIGURE 2.** Diffractogram of pillared clay using  $\text{TiCl}_4$  (a) without calcination process, (b) temperature calcination 200 °C, (c) calcination temperature 250 °C and (d) calcination temperature 300°C

## Impregnation using TiO<sub>2</sub>

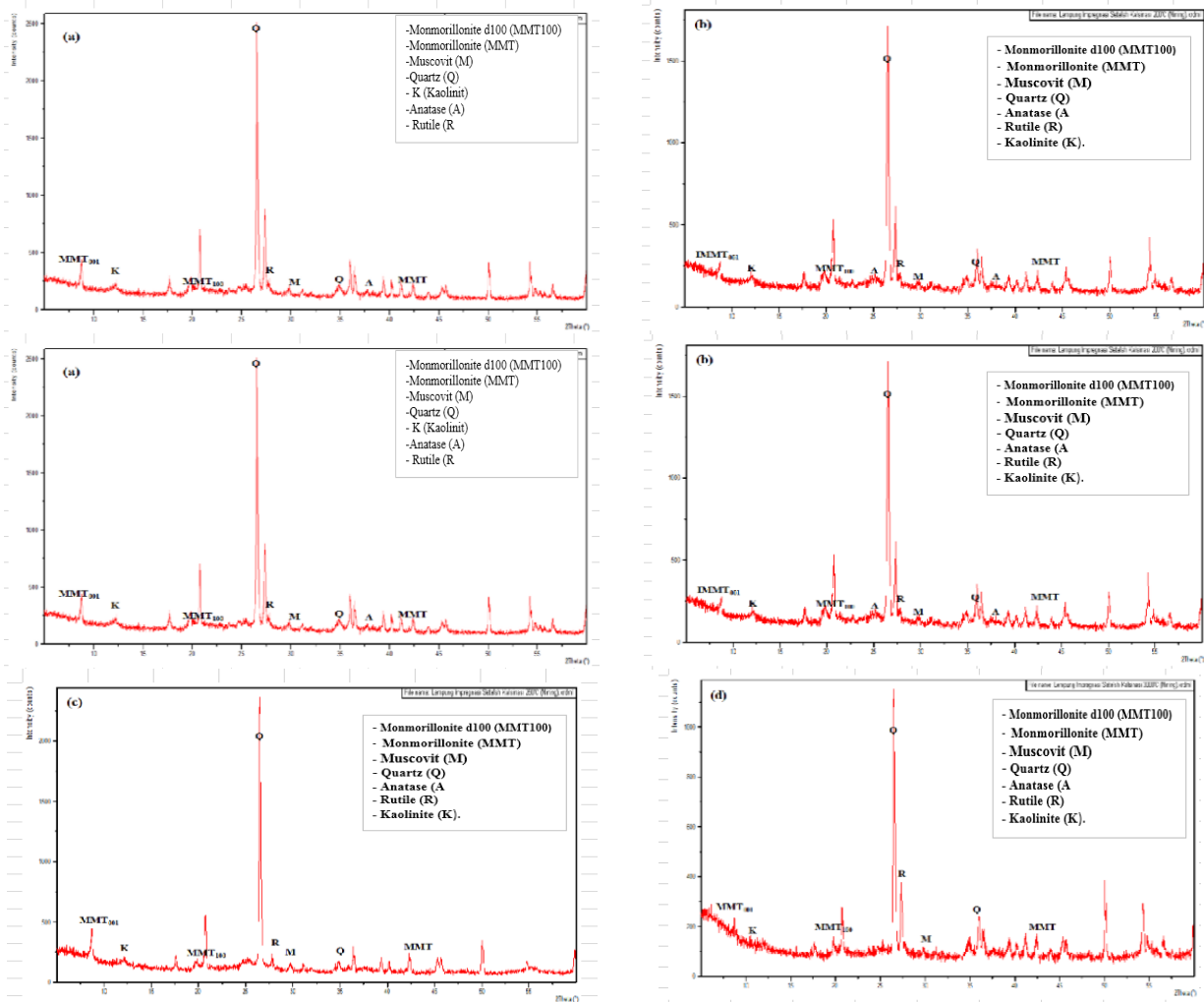


**FIGURE 3.** Diffractogram of impregnated clay (a) using TiO<sub>2</sub> without calcination, (b) calcined 200°C, (c) calcined 250°C, and d calcined 300°C

### Characterization

X-ray diffraction analysis was carried out at a scan angle range ( $2\theta = 5\text{--}60^\circ$ ), with Cu radiation source. The analysis was carried out to determine the changes in the structure of the clay after the pillaring process with TiCl<sub>4</sub> as a pillaring agent as well as the crystal phase of titanium in the clay interlayer which was applied without the calcination process and the variation of the calcination temperature of 200, 250, and 300°C. The characterization results are shown in Fig. 3.

The phenomenon of pillarization was observed using X-ray diffraction (Fig.2). The reflection of montmorillonite and other components in the treatment without calcination can be seen in Table 1, the 200°C calcination can be seen in Table 2, the 250°C calcination can be seen in Table 3, and the 300°C calcination can be seen in Table 4. Characterization using diffraction X-rays to determine crystallinity, identify phases and constituent components.

**TABLE 1.** Interpretation of the polarized clay diffractogram using TiCl<sub>4</sub> without calcination

Position 2θ (°)	d-spacing [Å]	Description
8,7842	10,06682	Monmorillonite (d <sub>001</sub> )
12,3147	7,18758	Kaolinite (d <sub>001</sub> )
19,8384	4,47636	Monmorillonite (d <sub>100</sub> )
26,6014	3,34823	Quartz
29,8563	3,20571	Muscovit
35,0330	2,55930	Quartz
42,4692	2,12680	Monmorillonite

Table 1 data refer to Fig. 2(a) montmorillonite reflection appears at plane diffraction angle (d<sub>001</sub>) (2θ) 8.7842 with d-spacing 10.06682 Å; the plane diffraction angle (d<sub>100</sub>) (2θ) was 19.8343 with d-spacing 4.47636 Å, and the diffraction angle (2θ) was 42.4692 with d-spacing 2.12680 Å. Multiple reflection angles of kaolinite, muscovite, and quartz. Table 2 refers to Fig. 2(b) where the montmorillonite reflection appears at the plane diffraction angle (d<sub>001</sub>) (2θ) 8.8065 with d-spacing 10.04139 Å; plane diffraction angle (d<sub>100</sub>) (2θ) 19.8805 with d-spacing 4.46607 Å; and at a diffraction angle (2θ) 42.4887 d-spacing 2.12763 Å. Some reflection angles of kaolinite, muscovite, and quartz are shown in Table 2.

**TABLE 2.** Interpretation of the polarized clay diffractogram using TiCl<sub>4</sub> calcination temperature 200°C

Position 2θ (°)	d-spacing [Å]	Description
8,8545	9,98708	Monmorillonite (d <sub>001</sub> )
12,1479	7,28593	Kaolinite (d <sub>001</sub> )
19,8805	4,46607	Monmorillonite (d <sub>100</sub> )
26,6379	3,34650	Quartz
29,9535	2,98319	Muscovit
35,0883	2,55751	Quartz
42,4887	2,12763	Monmorillonite

Table 3 data refers to Fig. 2(c) showing the reflection of montmorillonite at the plane diffraction angle (d<sub>001</sub>) (2θ) 8.8311 with d-spacing 10.01354 Å; plane diffraction angle (d<sub>100</sub>) (2θ) 19.8341 with d-spacing 4.47640 Å; and observed at a diffraction angle (2θ) 42.4977 d-spacing 2.12544 Å. A new reflection angle appears at the diffraction angle (2θ) 48.19656 d-spacing 1.88662. Some reflection angles of kaolinite, muscovite, and quartz are shown in Table 3.

**TABLE 3.** Interpretation of polarized clay diffractogram using TiO<sub>2</sub> calcination temperature 250°C

Position 2θ (°)	d-spacing [Å]	Description
8,8065	10,04139	Monmorillonite (d <sub>001</sub> )
12,3460	7,16943	Kaolinite (d <sub>001</sub> )
19,8341	4,47640	Monmorillonite (d <sub>100</sub> )
26,6130	3,34679	Quartz
29,9500	2,98106	Muscovit
35,9420	2,49663	Quartz
42,4977	2,12544	Monmorillonite
48,1966	1,88662	Titanium Oxide

Table 4 data referring to Fig. 2(d), montmorillonite reflection appears at plane diffraction angle (d<sub>001</sub>) (2θ) 8.8311 with d-spacing 10.01354 Å; plane diffraction angle (d<sub>100</sub>) (2θ) 19.8390 with d-spacing 4.47530 Å; and observed at a diffraction angle (2θ) 42.3944 d-spacing 2.13214 Å. Some reflection angles of kaolinite, muscovite, and quartz are shown in Table 4.



**TABLE 4.** Interpretation of the polarized clay diffractogram using a calcination temperature of 300 °C

Position 2θ (°)	d-spacing [Å]	Description
8,8311	10,01354	Monmorillonite (d <sub>001</sub> )
12,3236	7,18241	Kaolinite (d <sub>001</sub> )
19,8390	4,47530	Monmorillonite (d <sub>100</sub> )
26,5470	3,35775	Quartz
29,8193	2,99631	Muscovit
35,9660	2,49709	Quartz
42,3944	2,13214	Monmorillonite

The effect of calcination temperature on the montmorillonite phase can change the reflection angle and d-spacing of the pillared clay. Clay without calcination treatment up to 300°C gives different reflection angles and d-spacing. The highest reflection angle is shown at a calcination temperature of 200°C which is 8.85 with the lowest d-spacing of 9.99Å while the lowest reflection angle is shown without calcination treatment of 8.78 with the largest d-spacing of 10.07Å. The peak characteristic of montmorillonite in clay after preparation according to Teddy (2018) is at an angle of 19.866 with a d-spacing of 4.4656 Å, with a sufficiently large d-spacing clay can be used as an adsorbent and has no photocatalytic ability, because the metal oxide shearing process does not occur. At a calcination temperature of 200°C, the pillars have not been fully formed so that they have a small Bacal spacing. The Bacal spacing changed at 250°C calcination because the titanium oxide pillars have been formed, but decreased at 300°C calcination temperature, thus it can be concluded that the thermal stability of titanium pillared clay is at a temperature of 250°C. The more shifted to the left the reflection angle, the better this is because shifting to the left can increase the d-spacing. The shift is caused by the thermal effect of calcination so that it affects the stability of the clay lattice and changes the reflection value of the clay. Inconsistent increase in d-spacing indicates the pillaring process is not going well. The success of the pillarization process can be seen by the specific absorption of MMT-TiO<sub>2</sub> which is shown in Table 5 which refers to Fig. 2. The reflection peaks that appear correspond to the reflection peaks of the rutile and anatase of TiO<sub>2</sub> crystal phases thus it can be seen that polarized clay using TiCl<sub>4</sub> is a combination of anatase and rutile crystal phases. The reflection peaks can be seen in Table 5.

**TABLE 5.** The arrangement of the reflection peaks of the MMT-TiO<sub>2</sub> crystalline phase on polarized clay using TiCl<sub>4</sub>

Theoretical*		LP 0		LP 200		LP 250		LP 300	
2θ	Desc.	2θ	Desc.	2θ	Desc.	2θ	Desc.	2θ	Desc.
25,40	Anatase	25,54	Anatase	-	-	25,52	Anatase	25,47	Anatase
27,86	Rutile	27,81	Rutile	27,89	Rutile	27,79	Rutile	27,82	Rutile
37,70	Anatase	37,79	Anatase	-	-	37,72	Anatase	37,71	Anatase
48,34	Anatase	-	-	-	-	48,1956	Anatase	-	-
55,00	Anatase	-	-	55,41	Anatase	54,9	Anatase	-	-

The calcination process plays a very important role in the pillaring process between layers of clay. It can be observed several TiO<sub>2</sub> reflection peaks in TiO<sub>2</sub> pillared clay. After preparation of the clay, no reflections of the titanium phase were found. The pillared clay using TiCl<sub>4</sub> at a calcination temperature of 200°C has only one reflection peak of anatase TiO<sub>2</sub> and rutile TiO<sub>2</sub>. This is because at the calcination temperature the pillars formed are not yet perfect. At a calcination temperature of 250°C three anatase peaks and one rutile appeared. This is because at this calcination temperature a perfect pillar has formed. At higher heating, which is 300°C, the peak of the anatase TiO<sub>2</sub> reflection shifts and something disappears this is due to the pillar collapsing

### Impregnation using TiO<sub>2</sub>

Improving the performance of the clay can be done by modifying it using the wet impregnation method. The impregnation in this process was dissolved using absolute ethanol and the impregnator used was TiO<sub>2</sub>. The activated clay was mixed at once with TiO<sub>2</sub> and absolute ethanol, then stirred for 4 hours to ensure that the TiO<sub>2</sub> was

homogeneous on the surface of the clay. The mixture is then dried to evaporate the solvent, then the calcination process is carried out with temperature variations of 200, 250, and 300°C. The calcination process aims to activate the TiO<sub>2</sub> catalyst and to determine the thermal stability of the impregnated clay and its ability as photocatalyst in degrading surfactants. Vissully, clay after calcination does not have a specific color difference, due to heating on does not change the composition of the clay so much does that it not in change physical and chemical properties of the clay [13-16]. The analysis done using x-ray diffraction is to determine change in the clay structure after impregnation, the success impregnator distribution on the clay surface and to observe the phase change in titanium due to calcination treatment. The result of x- ray diffraction characterization are show in Fig. 3

The impregnation process using TiO<sub>2</sub> with variations in calcination temperature did not change the overall structure of the clay, the clay just had a shift in value of 2θ for each calcination treatment, this was evidenced by the characteristic peaks of montmorillonite in the diffractogram results. The treatment without calcination can be seen in Table 6, calcination of 200°C can be seen in Table 7, calcination of 250°C can be seen in Table 8 and calcination of 300°C can be seen in Table 9.

**TABLE 6.** Interpretation of impregnated clay diffractogram using TiO<sub>2</sub> without calcination

Position 2θ (°)	d-spacing [Å]	Description
8,7504	10,10571	Monmorillonite (d <sub>001</sub> )
12,2332	7,23532	Kaolinite (d <sub>001</sub> )
19,8164	4,48036	Monmorillonite (d <sub>100</sub> )
26,5324	3,35956	Quartz
29,8234	2,99590	Muscovit
35,9657	2,49710	Quartz
42,3762	2,13301	Monmorillonite

Table 6 data refer to Fig. 3(a) montmorillonite reflection appears at a plane diffraction angle (d<sub>001</sub>) (2θ) 8.7504 with d-spacing 10.10571 Å, diffraction angle (d<sub>100</sub>) (2θ) 19.8164 with d-spacing 4.48036 Å and observed at a diffraction angle (2θ) 42.3762 d-spacing 2.13301 several reflection angles of kaolinite, muscovite, and quartz.

**TABLE 7.** Interpretation of impregnated clay diffractogram using TiO<sub>2</sub> calcination at the temperature of 200°C

Position 2θ (°)	d-spacing [Å]	Description
8,7474	10,10919	Monmorillonite (d <sub>001</sub> )
12,2062	7,25127	Kaolinite (d <sub>001</sub> )
19,7297	4,49986	Monmorillonite (d <sub>100</sub> )
26,5513	3,35722	Quartz
29,7998	2,99823	Muscovit
35,9891	2,49554	Quartz
42,3612	2,13197	Monmorillonite

Table 7 data refer to Fig. 3(b) showing the montmorillonite reflection at plane diffraction angle (d<sub>001</sub>) (2θ) 8.7474 with d-spacing 10.10919 Å, plane diffraction angle (d<sub>100</sub>) (2θ) 19.7297 with d-spacing 4.49986 Å, and at a diffraction angle (2θ) 42.3612 with d-spacing 2.131997 Å, multiple reflection angles of kaolinite, muscovite, and quartz (see Table 8).

Table 8 refers to Fig. 3(c) showing the montmorillonite reflection at plane diffraction angle (d<sub>001</sub>) 8.7241 with d-spacing 10.13609 Å, plane diffraction angle (d<sub>100</sub>) (2θ) 19.7453 with d-spacing 4.49634 Å and observed at a diffraction angle (2θ) 42.3379 with d-spacing 2.13485 Å, multiple reflection angles of kaolonit, muscovite, and quartz (see Table 9).

**TABLE 8.** Interpretation of impregnated clay diffractogram using TiO<sub>2</sub> calcination at a temperature of 250°C

Position 2θ (°)	d-spacing [Å]	Description
8,7241	10,13609	Monmorillonite (d <sub>001</sub> )
12,1980	7,25609	Kaolinite (d <sub>001</sub> )
19,7453	4,49634	Monmorillonite (d <sub>100</sub> )
26,4954	3,36417	Quartz
29,7569	3,00245	Muscovit
35,8866	2,50242	Quartz
42,3379	2,13485	Monmorillonite

**TABLE 9.** Interpretation of impregnated clay diffractogram using TiO<sub>2</sub> calcination at a temperature of 300°C

Position 2θ (°)	d-spacing [Å]	Description
8,7716	10,08135	Monmorillonite (d <sub>001</sub> )
11,8988	7,43786	Kaolinite (d <sub>001</sub> )
19,7402	4,49750	Monmorillonite (d <sub>100</sub> )
26,4594	3,36867	Quartz
29,7688	3,00127	Muscovit
35,9623	2,49733	Quartz
42,3115	2,13613	Monmorillonite

Table 9 data refer to Fig. 3(d) showing montmorillonite at plane diffraction angle (d<sub>001</sub>) 8.7716 with d-spacing 10.08135 Å, plane diffraction angle (d<sub>100</sub>) (2θ) 19.8164 with d-spacing 4.48036 Å, and observed at a diffraction angle (2θ) 42.3762 with d-spacing 2.13301 Å multiple reflection angles of kaolinite, muscovite, and quartz. The effect of calcination temperature on the montmorillonite phase can change the reflection angle and d-spacing of the impregnated clay. At a calcination temperature of 200°C the catalyst was better than the calcination of 250, 300, and without calcination treatment. It is indicated in this condition that agglomeration occurs, causing the TiO<sub>2</sub> to be uneven on the clay surface. Thus it can be concluded that the thermal stability of the impregnated TiO<sub>2</sub> clay occurred at a temperature of 200°C. The more shifted to the left the angle of reflection the better. The shift is caused by the thermal effect of calcination so that it affects the distribution of TiO<sub>2</sub> in the clay lattice clay and changes its reflection value. The success of the impregnation process is known by the appearance of MMT-TiO<sub>2</sub> absorption which is shown in Table 10. The reflection appears according to the reflection of the rutile and anatase TiO<sub>2</sub> crystal phases so that it can be seen that the impregnated clay using TiO<sub>2</sub> is a combination of anatase and rutile crystal phases, the reflection can be seen in Table 10.

**TABLE 10.** Arrangement of MMT-TiO<sub>2</sub> crystal phase reflection peaks on clay impregnated using TiO<sub>2</sub>

Theoretical *		LT 0		LT 200		LT 250		LT 300	
2θ	Desc.	2θ	Desc.	2θ	Desc.	2θ	Desc.	2θ	Desc.
25,40	Anatase	-	-	25,37	Anatase	-	-	-	-
27,86	Rutil	27,79	Rutil	27,83	Rutil	27,78	Rutil	27,82	Rutil
37,70	Anatase	37,67	Anatase	37,54	Anatase	-	-	-	-
48,34	Anatase	-	-	-	-	-	-	-	-

The appearance of the most TiO<sub>2</sub> phase was in impregnation with a calcination temperature of 200°C, at a calcination temperature of 250°C, 300°C, and without calcination did not show a reflection at an angle of 25.40 this was probably due to the poor distribution of TiO<sub>2</sub> and calcination in this condition was unable to convert TiO<sub>2</sub> to its anatase phase. Calcination of 200°C was able to convert TiO<sub>2</sub> to the anatase and rutile phases so that the impregnation of TiO<sub>2</sub> at this temperature resulted in the formation of more TiO<sub>2</sub> crystal phases. From the reflection of TiO<sub>2</sub> crystals, it can be seen that the higher the calcination temperature, the lower the peak of the TiO<sub>2</sub> crystal reflection. This is due to the thermal effect of calcination affecting the crystallinity of TiO<sub>2</sub>.

## Surfactant Degradation

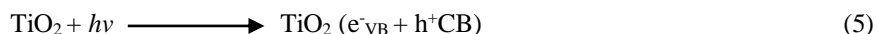
Before measuring the absorbance of LAS degradation results, the maximum wavelength ( $\lambda_{max}$ ) was measured. Measurements were carried out using a UV-Vis spectrophotometer at a wavelength of 500–670 nm. From the measurement results obtained a maximum wavelength of 650 nm. Based on the wavelength, it is used for the measurement of the MB-LAS standard curve. Colorless LAS surfactants need to be complexed (stained) so that the surfactants are colored so that changes in degradation can be observed using a UV-Vis spectrophotometer. The MBAS (Metylen Blue Active Surfactant) method is a complex method using methylene blue which is directly bonded to a hydrophobic LAS using the solvent extraction principle. Solvent extraction is based on the principle of distribution of substances based on the solubility of the solvent used, methylene blue bound to LAS can be extracted using chloroform because MB-LAS is soluble in chloroform.

The degradation process was carried out in a photocatalytic reactor for 1 hour with the help of radiation in the form of a 3x8 watt UV lamp. In the degradation system,  $H_2O_2$  is added before the degradation process (irradiated), the function of adding  $H_2O_2$  is as an irreversible electron acceptor and a source of OH radicals. The results of the degradation can be seen in Table 11.

TABLE 11. LAS surfactant degradation results in various treatments.

Type of treatment	Absorbance	$C_o$ (ppm)	$C_e$ (ppm)	$C_o - C_e$ (ppm)	D (%)
LP 0	0,361	2	0,819	1,181	59,05
LP 200	0,124	2	0,359	1,641	82,05
LP 250	0,097	2	0,216	1,784	89,20
LP 300	0,115	2	0,342	1,658	82,90
LT 0	0,434	2	0,961	1,039	51,95
LT 200	0,137	2	0,385	1,615	80,75
LT 250	0,206	2	0,519	1,481	74,05
LT 300	0,159	2	0,427	1,573	78,65

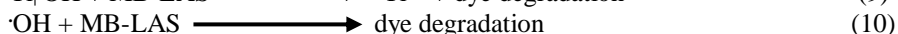
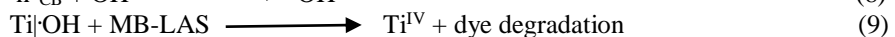
Based on the data, Table 11 shows that each treatment gave different results. The lowest percentage of degradation is shown in impregnated clay without calcination (LT 0) which is 51.95%, while the highest percentage of degradation is in pillared clay with a calcination temperature of 250°C (LP 250) which is 89.2%. The addition of catalyst in the degradation process gave significant results, LT 0 showed the lowest percentage of degradation is shown in impregnated clay without calcination (LT 0) which is 51.95%, while the highest percentage of degradation is in pillared clay with a calcination temperature of 250°C (LP 250) which is 89.2%. The addition of catalyst in the degradation process gave significant results, LT 0 showed the lowest percentage of degradation. This is possibly because in the impregnation process without calcination treatment  $TiO_2$  is less well distributed compared to LP 200 which has a better  $TiO_2$  distribution so that the formation of  $TiO_2$ -MMT pillars is better with the appearance of more  $TiO_2$  phases. The degradation process begins with the absorption of photons by  $TiO_2$  catalyst particles from UV light in the reactor. The pair of charge carriers, namely electrons ( $e^-_{VB}$ ) formed in the semiconductor and positive holes ( $h^+_{CB}$ ) will form on the surface of the semiconductor which is shown in the excitation reaction below:



$e^-_{VB}$  and  $h^+_{CB}$  will undergo recombination, i.e. return to their initial state and release photon energy as heat, then migrate to the surface and react with adsorbed compounds, as shown in the reaction (6).



In addition, hydroxide ions and water molecules form hydroxide radicals by binding to  $h^+_{CB}$ , the reaction can be seen in (7) and (8). Furthermore, the reaction on the solid-liquid surface hydroxyl radicals generated on the surface of  $TiO_2$  bind to MB-LAS molecules (9) or hydroxyl radicals diffuse into the solution and bind MB-LAS (10), as shown below:



Based on the surfactant degradation data in Table 11, the reduction in the concentration of degradation at LP 0 of 1.181 ppm was greater than that of LT 0 which was 1.039. This is due to the absence of catalyst activation, but the adsorption process of montmorillonite can reduce the dye because it can accumulate dye in the pores. These results indicate that LAO has a large adsorption capacity. The greater the adsorption ability, the better the degradation process, the higher the reduction concentration of MB-LAS

The degradation treatment with pillared clay with temperature variations showed good performance in the degradation of LP 250. This was due to the calcination process at a temperature of 250 to form good pillars thus the degradation process using TiO<sub>2</sub> pillared clay gave a degradation percentage of 89% with an adsorption capacity of 0.357 mg/g (the largest percentage of degradation) as shown in Table 5 which has the most occurrences of MMT-TiO<sub>2</sub>, namely four MMT-TiO<sub>2</sub> anatase and one MMT-TiO<sub>2</sub> rutile while pillarization at a temperature of 200°C (LP 200) with an adsorption capacity of 0.328 mg/g has a lower percentage of degradation that is equal to 82.05% with a capacity of 82.905%. adsorption of 0.332 mg/g. At 200°C (LT 200) impregnated clay, the percentage of degradation was greater than without calcined (LT 0) calcined 250 (LT 250), and calcined 300°C (LT 300). LT 200 provides good color degradation performance of 80.75% with an adsorption capacity of 0.323 mg/g as shown in Table 10 which has the appearance of MMT-TiO<sub>2</sub>, namely two MMT-TiO<sub>2</sub> anatase and one MMT-TiO<sub>2</sub> rutile compared to LT 250 of 74.05% with adsorption capacity of 0.296 mg/g and LT 300 of 78.65% with adsorption capacity of 0.315 mg/g which only had MMT-TiO<sub>2</sub> rutile. LT 200 degradation showed good performance because at 20°C calcination it was possible for TiO<sub>2</sub> to be well distributed, but at 250°C and 300°C calcination occurred agglomeration thus TiO<sub>2</sub> was not well distributed. The results of MB-LAS degradation can be seen in Fig.3.

The color degradation ability of MB-LAS is better using TiO<sub>2</sub>-pillared clay than TiO<sub>2</sub> impregnated clay, this is indicated by the peak reflection of the MMT-TiO<sub>2</sub> phase in Table 5 and Table 10. The highest percentage of degradation in the clay pillarization method is shown in LP 250 and the impregnation method in The LT 200. LT 200 has three reflections with two anatase reflections and one rutile reflection. According Afrozi and Sudaryanto (2016), due to having five TiO<sub>2</sub> reflections with four anatase reflections and one rutile reflection, the anatase phase plays a very important role in the degradation process, the anatase TiO<sub>2</sub> crystal phase is the stable and most reactive TiO<sub>2</sub> phase to light because it has an energy band gap of 3, 2 eV (380 nm) therefore the excitation of electrons to the conduction band can easily occur when exposed to light with an energy greater than the gap energy. Meanwhile, rutile crystals are formed from anatase crystal transformation with a band gap of 3.0 eV (415 nm).

## CONCLUSION

Synthesis and characterization of x-ray diffraction of pillared clay using TiCl<sub>4</sub> and impregnated using TiO<sub>2</sub> containing components of kaolinite, muscovite, quartz and montmorillonite. The resulting pillared clay has a calcination thermal stability of 250°C with four occurrences of MMT-TiO<sub>2</sub> anatase and one occurrence of MMT-TiO<sub>2</sub> rutile. The resulting impregnated has a calcination thermal stability of 200°C with two occurrences of MMT-TiO<sub>2</sub> anatase and one occurrence of MMT-TiO<sub>2</sub> rutile. The degradation performance of Linear Alkylbenzene Sulfonate with the largest photocatalyst of pillared clay using TiCl<sub>4</sub> was shown at a calcination temperature of 250°C at 89.20% with an adsorption capacity of 0.357 mg/g and the largest impregnated clay using TiO<sub>2</sub> was shown at a calcination temperature of 200°C at 80.75%. adsorption capacity of 0.323 mg/g.

## ACKNOWLEDGMENTS

Through the writings of the main authors and members, they express their gratitude to the Southeast Sulawesi government, especially the Kendari city government in tackling and preventing the transmission of Covid 19 by inviting the public to obey the health protocol regulations (PROKES)

## REFERENCES

1. C. Bijang, A. W. Wahab, A. Ahmad, and P. Taba, *Int. J. Mater. Sci. Appl.* **4** (2015)
2. N. Binitha and S. Sugunan, *Journal Pre-proof.* **93**, (2006).
3. M. Baizig, S. Khalfallah, B. Jamoussi, N. Batis, and R. Trujillano, *IJEScA* **4** (2015)
4. D. E. Santiago, M. Hernández Rodríguez, and E. Pulido-Melián, *J. Environ. Eng.* **147** (2021).
5. E. T. Wahyuni, R. Roto, M. Sabrina, V. Anggraini, N. Leswana, and A. Vionita, *J. Appl. Chem.* **4** (2016).
6. S. Suriani, S. Suharjono, and S. Soemarno, *J. Environ and Sust Develop* **6**, (2015)
7. B. Hampel, Z. Pap, A. Sapi, A. Szamosvolgyi, L. Baia, and K. Hernadi, *Catalysts* **10** (2020).
8. S. Fatimah and A. Haris, *J. Shem. Sci. and Appl.* **50** (2010).
9. S. J. Sekewael, Chemistry Study Program, Department of Chemistry, Faculty of Mathematics and Natural Sciences, UGM, Yogyakarta (2017)
10. K. H. Tan, *Fundamentals of Soil Chemistry* (First Edition, translating Goenadi, D. H., Gadjah Mada University Press, Yogyakarta, 1982).
11. M. Sychev, T. Shubina, M. Rozwadowski, A. P. B. Sommen, V. H. J. D. Beer, and R. A.V. Santen, *J. Microp. and Mesops. Mater* **37**, 187–200 (200).
12. O. C. J. Van and R. F. J. Giese, *Disper Sci. and Tech.* **24** (2003),
13. P. Monvisade and P. Siriphanon, *J. Appl. Clay. Sci.* **24**, 427–431 (2009).
14. J. Orthman, *Individual Inquiry* (University Of Queensland, Brisbane, (2000).
15. H. Gecol, P. Miakatsindila, E. Ergican, and S. R. Hiibel, *Desalination* **197**, 643-651 (2006)
16. P. Banković, A. Milutinović-Nikolić, Z. Mojović, N. Jović-Jovičić, J. Dostanić, Z. C. Lončarević, and D. Anović, *J. Act. Phys. Polon.* **115(4)**, (2009).